Published online 26 March 2012

Nucleic Acids Research, 2012, Vol. 40, No. 13 ***e99***
doi:10.1093/nar/gks276

Single-stranded loops as end-label polarity markers for double-stranded linear DNA templates in atomic force microscopy

Daniel J. Billingsley[1,2], Neal Crampton[1], Jennifer Kirkham[2], Neil H. Thomson[1,2] and William A. Bonass[2,*]

[1]School of Physics and Astronomy and [2]Department of Oral Biology, Leeds Dental Institute, University of Leeds, Woodhouse Lane, Leeds, West Yorkshire, LS2 9JT, UK

Received January 30, 2012; Revised and Accepted March 13, 2012

ABSTRACT

Visualization of DNA–protein interactions by atomic force microscopy (AFM) has deepened our understanding of molecular processes such as DNA transcription. Interpretation of systems where more than one protein acts on a single template, however, is complicated by protein molecules migrating along the DNA. Single-molecule AFM imaging experiments can reveal more information if the polarity of the template can be determined. A nucleic acid-based approach to end-labelling is desirable because it does not compromise the sample preparation procedures for biomolecular AFM. Here, we report a method involving oligonucleotide loop-primed synthesis for the end labelling of double-stranded DNA to discriminate the polarity of linear templates at the single-molecule level. Single-stranded oligonucleotide primers were designed to allow loop formation while retaining 3′-single-strand extensions to facilitate primer annealing to the template. Following a DNA polymerase extension, the labelled templates were shown to have the ability to form open promoter complexes on a model nested gene template using two *Escherichia coli* RNA polymerases in a convergent transcription arrangement. Analysis of the AFM images indicates that the added loops have no effect on the ability of the promoters to recruit RNA polymerase. This labelling strategy is proposed as a generic methodology for end-labelling linear DNA for studying DNA–protein interactions by AFM.

INTRODUCTION

Atomic force microscopy (AFM) is an important single-molecule technique, and thus offers advantages over more traditional ensemble biochemical methodologies. It is possible to observe each member of the population under study individually, and thereby obtain an overall distribution of results. AFM directly visualizes single molecules with high signal-to-noise and has the added advantage that sample preparation is relatively quick and simple. DNA can be imaged on its own or in complexes with other biomacromolecules, e.g. proteins, by deposition onto atomically flat hydrophilic mineral surfaces such as mica (or modified mica). The instrument's versatility is highlighted by the wide range of studies with regard to DNA alone that the technique has permitted, including studies into DNA structure, supercoiling and condensation (1–3).

In particular, the technique has allowed the interaction of a range of different proteins with DNA templates to be studied, including RNA polymerase (RNAP), transcription factors, nucleosomes and restriction endonucleases (4–12). DNA is easily identifiable by its semi-flexible chain morphology, with bound proteins having a globular structure. The method has enabled important information about the spatial arrangements of DNA and protein, such as bending, wrapping and looping to be obtained (10,13,14). Dynamic processes such as transcription elongation can also be followed by imaging in bulk aqueous liquid (15).

Generally, for structural studies, DNA–protein complexes are formed *in vitro*, before incubation onto a supporting surface, before being dried and imaged under air. Under these conditions, it becomes necessary to verify that the population under study represent specific protein–DNA interactions. Interactions between DNA and

*To whom correspondence should be addressed. Tel: +44 113 3436184; Fax: +44 113 3436548; Email: w.a.bonass@leeds.ac.uk

proteins can be denoted as specific by performing contour length measurements of the proteins' position from the ends of the template, and comparing these values with the expected binding site positions from the DNA sequence.

To date, studies of DNA transcription with AFM have generally used fairly simple model systems, typically consisting of short DNA templates containing the required binding sites (e.g. promoter or stall site) and the relevant protein under study. However the situation *in vivo* is much more complex; for example with regard to transcription, genes can be thousands of base pairs long, and a RNAP may require a number of different transcription factors to assist activation of transcription. This method of contour length measurements is viable for multiple proteins on a template providing that there is some degree of asymmetry in the positions of the respective binding sites.

However, attempts to study dynamic interactions between more than one protein moving along a single template (for example RNAPs originating from different promoter sites) is difficult as once they move away from their initial binding site, it is not possible to unequivocally determine the starting point of each protein. End-labelling the DNA template, can resolve this issue, by providing a means to determine the polarity of the DNA in the AFM. If multiple proteins travelling along a single DNA template cannot pass each other, the individual proteins can be identified by their relative positions to each other and the end label. Interactions that are more complex, and involve transient unbinding from the DNA, such as hopping and inter-segment transfer, will require direct labels on the protein, however, this approach is beyond the scope of this method. The end-labelling strategy described here is particularly suitable for processive motions of molecular motors, such as helicases and polymerases.

Typically, dynamic AFM provides a topographical map of the surface (16), therefore DNA molecular end-labels must be identifiable by a size difference with respect to the DNA chain width. Linear DNA has previously been end-labelled with proteins by incorporating biotinylated nucleotide triphosphates (NTPs) into the chain, which can then be complexed with the protein streptavidin (17–19) or a streptavidin–gold conjugate (20). A drawback of using these techniques with AFM arises because these protein labels can affect the binding of the DNA complex to the surface. We previously trialled an approach of attaching streptavidin to the end of a biotinylated DNA and found that the efficiency of labelling was only 10% and that it affected the 3D to 2D equilibration of DNA onto the mica surface (21). Other proteins may not cause these issues (22) but the buffers for AFM sample preparation and operation are optimized to control DNA binding and therefore a nucleic acid-based approach is generic. If non-specific protein–protein interactions occur between the end-label protein and the enzyme of interest, they will influence the conformation of the DNA rendering determination of the relative positions of multiple proteins through morphological identification alone, difficult. Protein–protein interactions are affected by salt concentrations (23) and deposition of DNA–protein complexes for AFM is often carried out in low ionic strength buffers where non-specific interactions may be more dominant.

A nucleic acid-based label, therefore, is more desirable since it has the same surface chemistry as the labelled DNA and therefore does not influence the binding of DNA–protein complexes to the support surface. One such approach for labelling sequence-specific regions in the interior of a DNA plasmid has utilized DNA stem–loops where the loop hybridizes with a specific sequence in the dsDNA to form a DNA triplex (24,25). Different sized stems; one of 200 bps and one of 500 bps were utilized as the labels protruding from the plasmid to determine polarity. This method was optimized for electron microscopy rather than AFM and is ideal for circular DNA since triplex formation can be stabilized by DNA supercoiling (26). However, the sensitivity of triplex formation to supercoiling makes this approach unsuitable for linear DNA molecules.

We have developed a different strategy for linear DNA, in which a DNA stem–loop was incorporated into the chain at one end via covalent linkage of the stem and using the loop as the polarity marker. DNA–protein interactions by AFM are often carried out using linear templates because they are easier to prepare with no cross-overs on a 2D surface (22), and thereby visualize the whole backbone length. Typically, the length of the templates used is only around 1kbp to optimize throughput of image acquisition by AFM for statistical analysis.

Labelling with nucleotides alone, and without any ancillary proteins, allows unambiguous differentiation between the label and the DNA-binding protein under study. If labelling was performed using an additional protein marker at one end of a DNA molecule there is the additional disadvantage that it may interact non-specifically with the protein of interest, such as a polymerase undergoing 1D diffusion along the DNA, prior to formation of a promoter complex.

We tested the ability of this labelling technique to allow differentiation between two binding sites, using a DNA template containing two distinct promoter sites, both of which can recruit *E. coli* RNAP. The template was designed such that the promoter regions are asymmetrically situated. By achieving the labelling of a single template end, both RNAPs can be unequivocally identified and cross-referenced to their starting promoters, even after the initiation stage of transcription, thus facilitating interpretation of events which involve RNAP–RNAP interactions, previously obscured if an unlabelled template is used.

MATERIALS AND METHODS

Template construction

A single linear DNA template was used for both labelling reactions and to study subsequent DNA protein interactions. The template was obtained from the 6136-bp plasmid pDSU, containing two λ_{PR} promoters situated in a convergent arrangement, and separated by 338 bp. The plasmid underwent enzymatic digestion by HindIII

for 2 h at 37°C to release a linear fragment 1149 bps in length containing both promoter sites, plus three other extraneous fragments. Separation of the products was achieved by gel electrophoresis, the fragment of interest visualized under UV light as a discrete band, and subsequently excised from the gel and purified using the QIAquick Gel Extraction Kit (Qiagen, Valencia, CA, USA), as per the manufacturer's instructions.

End-labelling of template

The aim of this study was to attach a DNA stem–loop to one end of the 1149-bp HindIII-generated linear pDSU transcription template, such that it acted as an end-label. To this end, a single oligonucleotide stem–loop forming primer, having the sequence: 5′-GGCCCTGGAGGG*AAAAAAAAAAAAAAAAAA*ACCCTCCAGGGCC**GGTGGATCCAAGCTTAGGTGAGAACATCC-3′**, was used for single-cycle linear PCR (see Figure 1 for a summary). The bold bases represent the sequence that will anneal to the HindIII-digested fragment of pDSU, underlined sequences indicate inverted repeats that will hybridize to each other to form a stem, while the italics show the loop region. The oligonucleotide sequence was fed into the MFold DNA secondary structure prediction tool to check that it would fold into the structure expected (27).

Primer extension was performed using the GoTaq Hot Start Polymerase kit (Promega) by making up a 50 µl reaction mix containing the heat resistant *Taq* polymerase (2.5 U), template DNA (300 fmol), dNTP mix (1.6 mM of each dNTP) and $MgCl_2$ (4.0 mM). A 1000-fold excess of primer to template was used to encourage the labelling reaction to dominate over re-annealing (Figure 1.1). A denaturing step of 98°C for 10 min was initially performed, using all the reagents except the dNTPs and *Taq* polymerase to minimize heat damage (Figure 1.2). The higher than typical temperature and longer time period was used to ensure that the majority of the target was denatured, and also that the single-stranded regions diffuse away from their partner strands. The reaction mix was then immediately put on ice to encourage the stem–loop structure to form and to prevent re-annealing of the strands (Figure 1.3). At this stage, Taq polymerase and the dNTP mix was added. Following this, annealing was performed at 60°C for 10 min (Figure 1.4), and extension at 72°C for 15 min (Figure 1.5) in a single-cycle reaction. The PCR-generated fragments were purified using the QIAQuick PCR Purification Kit (Qiagen, Valencia, CA, USA), as per the manufacturer's instructions. See Figure 2 for a schematic diagram of the labelled fragment used in this study.

Preparation of transcription complexes

Once end-labelling was established, the technique was tested in a DNA–protein system. We examined the ability of the labelling reaction to study transcription complexes containing binding sites for more than one RNAP. *In vitro* transcription reactions were performed as previously described (14,28): 200 fmol of the labelled 1149-bp HindIII-digested fragment of pDSU (Figure 2a) was incubated at 37°C for 15 min with 400 fmol of *E. coli* σ^{70} holoenzyme (Epicentre), and 10 µl of transcription buffer [20 mM Tris–HCl (pH 7.9), 50 mM KCl, 5 mM $MgCl_2$, 1 mM DTT]. This reaction enables the formation of what are termed open promoter complexes (OPC). These consist of RNAPs that have formed specific interactions with the two promoter regions. Due to the absence of any NTPs in the reaction mix, the complexes are unable to enter the elongation stage of transcription, preventing production of nascent RNA chains.

The asymmetric location of the two promoter sites on the template defines three main DNA contour length measurements from AFM topographical images, for complexes containing two RNAPs bound at the respective promoters: the distance between the two RNAPs termed the inter-RNAP distance, and measurements from each RNAP to the chain end closest to it: the largest of which is termed the long-arm measurements, and the smallest the short-arm measurement (Figure 2b). The stem–loop forming oligonucleotide is designed with a structure such that the primer sequence anneals to the end of the long arm.

AFM

All reaction mixes were diluted 10-fold into imaging buffer [4 mM Tris–HCl (pH 7.5), 4 mM $MgCl_2$] to facilitate efficient binding to the support surface. Samples were deposited onto freshly cleaved muscovite mica (Agar Scientific) and left to incubate for 3 min at room

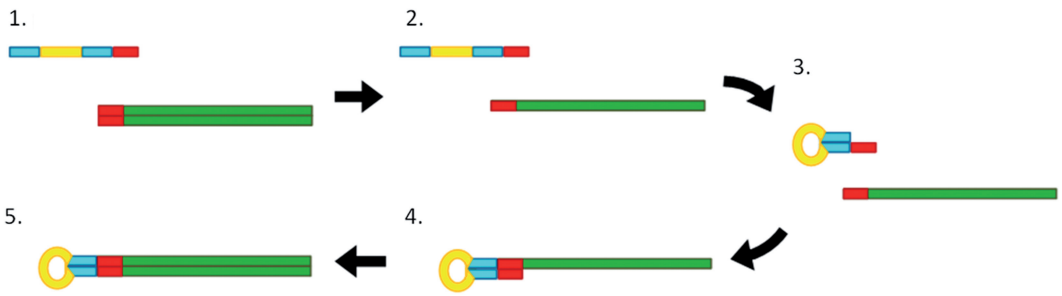

Figure 1. Summary of method used to end-label DNA, utilizing a PCR-based approach. Complementary base sequences are indicated by the same colour. The template is shown in green, while the stem and loop are highlighted in blue and yellow, respectively. Regions complementary on both the template and oligonucleotide are shown in red. It is this sequence that acts as a forward primer. (1) pDSU DNA template and primer. (2) Denaturing (98°C for 10 min). (3) Rapid cooling (formation of stem-loop). (4) Annealing (60°C for 10 minutes). (5) Extension (72°C for 15 min).

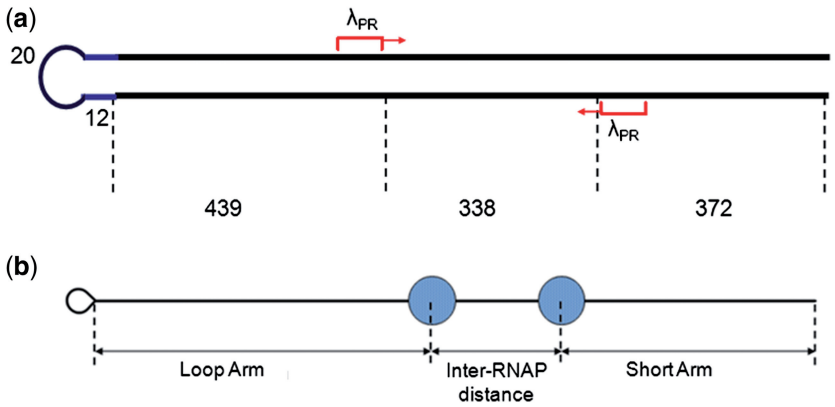

Figure 2. (**a**) Schematic representation of the template used in this study. It contains two λ_{PR} separated by around 338 bases. The numbers underneath display the number of base pairs present in certain regions of the template. The stem and loop are made up of 12 and 20 bases, respectively. (**b**) Schematic representation of the measurements taken during the analysis. The loop end-label is situated on what is termed the long arm.

temperature. Following this, samples were rinsed in Milli-Q water before being dried in a weak flux of nitrogen gas (1 bar pressure). AFM images were collected in air with a Multimode Nanoscope IIIa AFM (Veeco, Santa Barbara, CA, USA) operating in Tapping Mode using silicon cantilevers (Olympus, Tokyo, Japan) of quoted spring contant 42 Nm^{-1} and resonant frequency 300 kHz. Scans were collected at a scan line frequency of 2 Hz at 512×512 pixel resolution. Complexes were analysed in the Nanoscope software (Digital Instruments, Santa Barbara, CA, USA) and using ImageJ. Complexes containing two RNAPs bound to a single DNA were analysed in the following manner. Contour lengths were performed manually by following the DNA backbone as a series of connected straight lines. For studies into DNA–protein interactions three contour length measurements were taken: the short-arm distance, inter-RNAP distance, and the long-arm distance (Figure 2b). The 2D projection of the centre of mass of each RNAP was taken as the intersection between one measurement upstream of the template, and the next downstream.

RESULTS

Labelling reactions

Experiments were performed to allow the attachment of a stem–loop structure to the convergent transcription template, with the aim of end-labelling the chain and allowing each individual protein-binding sites to be better identified. Visualization of the stem–loop end-labelled DNA templates in the AFM, revealed a class of molecules that contained a feature at one end of template (see Figure 3 for a montage).

These appeared wider and often higher than the bulk of the DNA molecule. Average measurements of the width of the end feature and the main backbone were found to be 20.6 ± 0.4 and 12.7 ± 0.3 nm, respectively, while height measurements yielded averages of 1.05 ± 0.05 and 0.38 ± 0.02 nm. The feature appeared in various forms with a triangular shape being the most common ($P = 0.55$). Spherical ($P = 0.37$) and irregular or branched structures were also observed ($P = 0.08$) (Figure 4). This shows that the structure at the chain end has a certain degree of flexibility and can fold into different morphologies.

In order to qualify the success of the labelling reaction the complexes were categorized into three different groups: those with a globular feature at one end, those with no end feature and those with two end features. The fraction of molecules displaying a single feature at one end is a sign of how successful the labelling reaction has been.

Each AFM image contained a mixture of DNA that had a feature at the end of the chain and those that appeared to be unlabelled DNA (Figure 5). Using the labelling protocol described the number of end-labelled molecules observed was similar to those displaying no features ($P = 0.48$ versus $P = 0.50$, $n = 319$). Templates displaying two distinct end features proved to be rare ($P = 0.02$), and as such, unspecific labelling at the wrong end, i.e. the short arm, was not a problem. As a control, pDSU template that had not undergone end-labelling, had a much lower prevalence of molecules with an end feature ($P = 0.08$).

One might assume that the end feature would take the form of a ring when visualized with AFM. The lack of an inner hole could be for a number of reasons; insufficient imaging resolution due to the finite size of the AFM tip, preferential retention of salts from the imaging buffer within the loop during the sample preparation procedure, or non-specific interactions between the single strands of DNA in the loop when confined on a 2D surface.

To gain further proof that the end-labelling reaction had worked, or that the features observed were simply an effect of surface binding, contour length measurements were taken for the individual classes from the same scans. The average contour lengths for molecules that had no end feature and those that had one at a single end were 386 ± 3 and 407 ± 3 nm, respectively. The value for the unlabelled 1149-bp fragment (386 ± 3 nm) correlates to

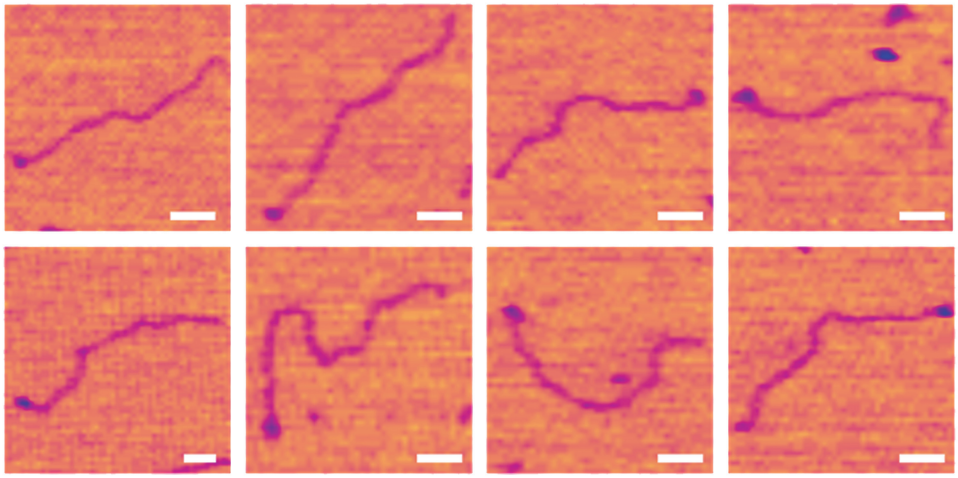

Figure 3. Montage showing software zooms of individual 1149 bp linear DNA molecules with a globular feature at one end: the stem–loop attached through the PCR reaction. Scale bars: 50 nm long.

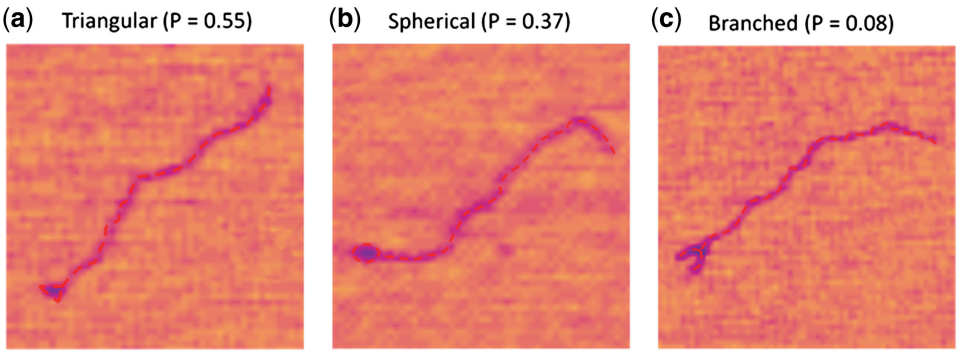

Figure 4. Examples of the different morphologies of end-loop structures, together with the relative occurrence of each class. Each molecule is traced out to highlight the differences in end structure.

a base pair repeat of 0.336 nm, a value typical of B-form DNA. These observations indicate that those templates with end features represent the results of a successful labelling reaction that is characterized by an increase in contour length. Such labelling is characterized by an increase in contour length (see distributions in Figure 6). Interestingly, the control DNA that appeared to have a feature at one end, but which had not gone through the labelling reaction had an average contour length of 344 ± 5 nm, significantly shorter than the expected length. In this case the blob feature on the end of the template is representative of a folding of the ends of the molecule or some other structural/morphological change, perhaps caused by some form of DNA condensation.

The longitudinal distance measured separately across the end feature was 20.5 ± 0.5 nm (Figure 7) and explains the extra contour length measured for templates with a loop feature. The loops appear larger than might be expected as the stem is only 12-bp long which one might expect to increase the size by only a few nanometres. Additionally, if it is assumed that the loop forms a roughly circular structure, consisting of 20 bases each separated by 0.33 nm, then this ring-structure would have a diametre of around 2 nm. However the single-stranded loop has a greater degree of flexibility than double-stranded regions, and as a result may be able to form varying secondary structures, which coupled with tip-convolution effects lead to a larger than expected end feature.

DNA–RNAP complexes

Once it became apparent that it was possible to attach the loop feature, thus labelling the molecule, the same labelled template was used to study actual DNA–protein complexes. The template contained two λ_{PR} promoters situated on opposite strands and separated by 338 bp. DNA–RNAP complexes were formed after incubation at 37°C of the protein with template DNA that had undergone the labelling reaction described above. The RNAPs are able to form stable interactions with the promoter regions, but due to the absence of NTPs are unable to move away from this position. Complexes were then bound to mica and imaged in ambient conditions with AFM.

A complex was denoted as an OPC if it contained two RNAPs positioned towards the centre of the template, and with a small separation consistent with the expected separation for the inter-promoter distance.

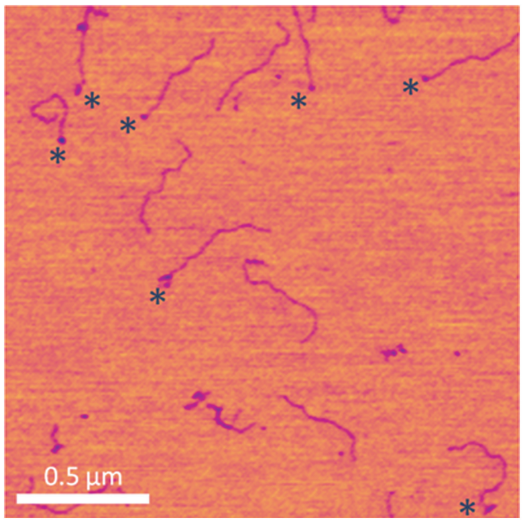

Figure 5. Example of a typical scan of the end-labelled 1149-bp linear DNA. Each image contained a mix of labelled and unlabelled complexes. Molecules that have a feature at a single end are marked by an asterisk.

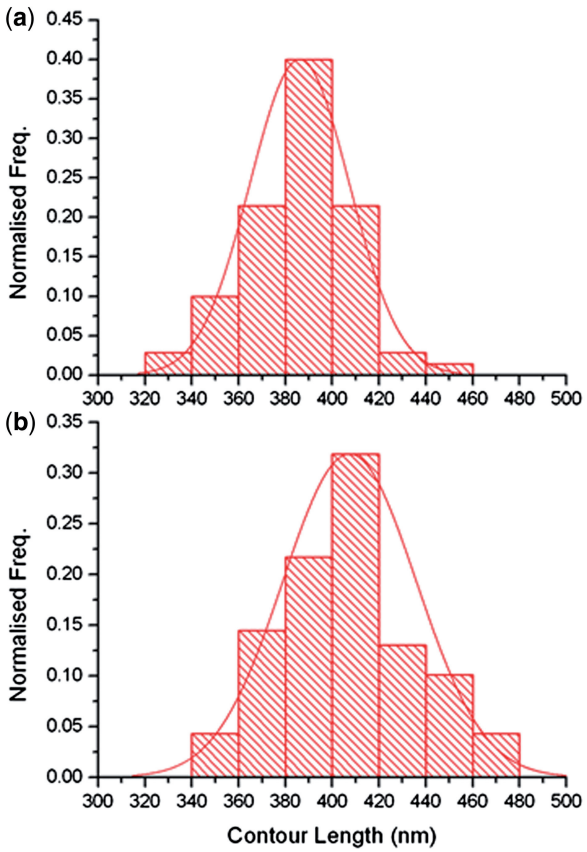

Figure 6. Contour length distributions for (**a**) bare DNA ($n = 69$) and (**b**) DNA with an end feature ($n = 74$). It appears that the labelling of the complex is characterized by an increase in total contour length. The average contour length increases by 21 nm once end-labelling has been performed.

Of the complexes containing two RNAPs, the holoenzymes were identified as being two equally sized globular structures situated in the central region of the template. A montage of labelled DNA molecules containing two

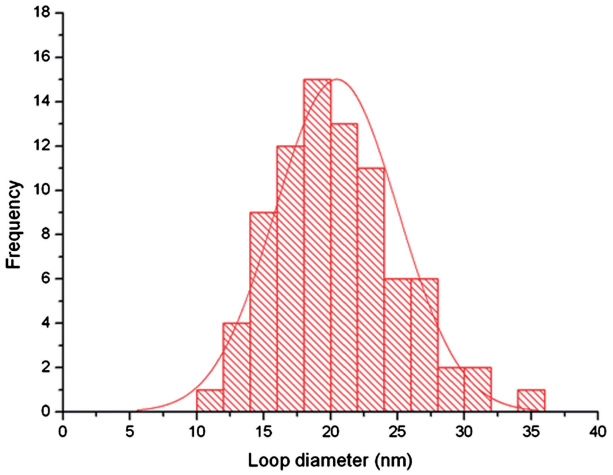

Figure 7. Distribution of diameter of the end feature ($n = 82$). The values are fitted to a Gaussian distribution corresponding to an average of 20.5 ± 0.5 nm. This measurement corresponds well with the extra contour length observed in molecules containing a feature at one end.

RNAPs, characteristic of OPCs is shown in Figure 8. These contain RNAPs bound in the position expected of the promoter. Such complexes also display the same globular feature at just a single end as seen previously. This shows that the presence of a loop structure at one end does not affect a proteins ability to locate and form interactions with its binding site.

The formation of DNA–RNAP complexes allows another control experiment concerning the end-labelling to be carried out. As the stem–loop is situated on what is termed the long-arm of the template, the other two measurements (the short-arm and inter-RNAP distance) should be unaffected by the presence of the stem–loop. In addition to this, of the end-labelled complexes, the distance from the loop to its nearest RNAP should be the larger of the two chain end to enzyme measurements. Table 1 summarizes the average values for the three main measurements, plus the contour length, for both labelled and unlabelled complexes. As expected there is little difference in the short-arm and inter-RNAP distances. The difference in the long-arm is 23 nm, which compares favourably with the measurements of the loop-feature diametre (20.5 ± 0.5 nm). Additionally, the loop feature was identified as being the long-arm in 86% of complexes with two RNAPs bound. The remaining complexes probably represent non-specific protein binding. The high level of success helps to display that such end-labelling of templates can be useful for correctly identifying protein-binding sites.

Relative to free DNA, the total contour length is reduced to 360 ± 6 nm (a reduction of 47 nm). This represents a reduction of 23.5 nm per bound RNAP. This is consistent with a model of DNA wrapping observed in similar AFM studies into *E. Coli* RNAP (14).

DISCUSSION

We pursued a technique for end-labelling DNA molecules for AFM using stem–loop forming oligonucleotides.

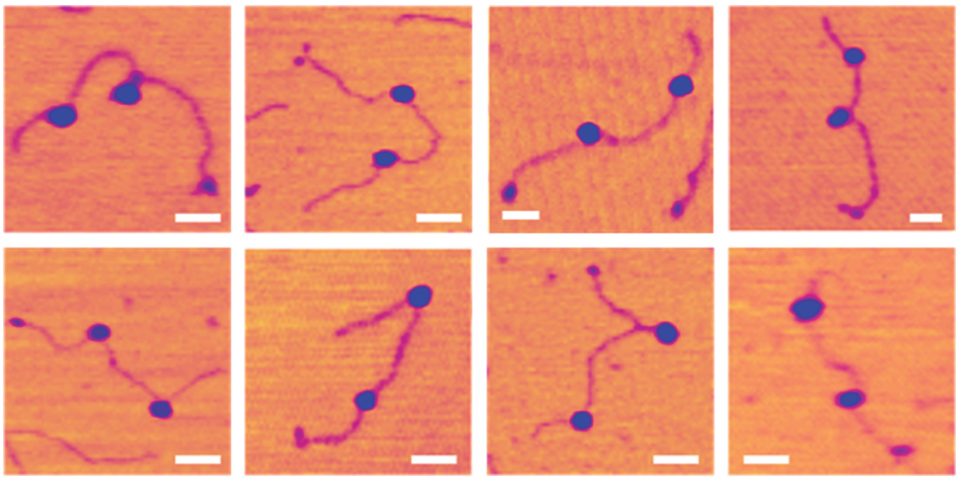

Figure 8. Montage of single-molecule software zooms depicting OPCs. The RNAPs are identified as two globular features, much wider than the chain width, and separated by a distance consistent with the inter-promoter length. Also visible is the loop feature at one end of the template. Scale bars: 50 nm.

Table 1. Comparison of length measurements for labelled and unlabelled OPCs

OPC sample (nm)	Short-arm (nm)	Inter-RNAP (nm)	Long-arm (loop) (nm)	Contour length (nm)
Unlabelled	91 ± 3	113 ± 6	127 ± 3	330 ± 4
Labelled	94 ± 4	115 ± 7	154 ± 5	360 ± 6

Through measurements of the DNA contour length, and the size of the end feature, a distinct population of molecules was identified, representing molecules, for which the PCR-derived labelling reaction had been successful, and thus contained a stem–loop at the expected end.

Ohta *et al.* studied (29) DNA promoters containing a palindromic nucleotide sequence with AFM. When imaging this sequence they observed a small feature at one end of the chain, and concluded that this was direct evidence of promoter based stem–loops. The features imaged in their study appeared very similar to those we observed in our study. The features they observed had a diametre of 10 nm for a loop consisting of 11 nt, while we observed a diametre of 20.5 ± 0.5 nm, with the increase in size correlating well with the higher number of bases in the loop (20 nt), providing further support that we observe stem–loops.

Yoshimura *et al.* (30) aimed to study how telomere repeat-binding factors (TRF) help to maintain telomeric DNA, by observing how the DNA complexed with the protein using AFM. They used DNA carrying a stretch of the sequence $(TTAGGG)_n$, and a long 3′-overhang, to represent telomeric DNA, and observed a number of higher order DNA structures at one end. These took the form of not only globular structures (a common sight in our labelled molecules), but also branched structures, a structure that we occasionally observed.

The stem–loop appeared broader and often higher than the main DNA backbone, and as such the labelled chain end was easily distinguishable from the other terminus. We were able to show that by using the present labelling method it was possible to distinguish between two different protein-binding sites, in this case *E. coli* RNAPs bound at two different promoters. The OPCs displayed a high degree of specificity with RNAP typically being seen in the positions expected, with the distance from the label to the RNAP being validated as being longer than the other arm-length. This confirms that the presence of the stem–loop does not hinder the activity of the protein, and its ability to form stable contacts with its binding sites.

Where end-labelled DNA fragments become especially useful is when the aim is to study dynamic interactions on a DNA template, when proteins move away from their initial binding sites. AFM has the ability to image processes *in situ* under bulk liquid or *ex situ* in ambient hydrating conditions on air-dried samples. This labelling strategy could be used in either situation to study processes involving protein translocation; for example promoter recognition, transcription elongation, convergent transcription and DNA digestion by restriction endonucleases (15,28,31–33). While fast scan AFMs are beginning to give the opportunity to infer the polarity of the DNA template during a process (32,34), scan speeds are still not always fast enough and direct labelling could greatly assist interpretation, although molecular motion under bulk aqueous liquid is always a concern.

Ex situ approaches on dried samples obviate molecular motion, and this strategy was previously used by our group to study a model convergent transcription system (28).The approach taken by Crampton *et al.* does have a major limitation on unlabelled templates. While it was possible to identify promoter-bound RNAPs readily, once the RNAPs 'fire' and begin to interact with one another, it becomes increasingly difficult to identify

which protein belonged to which promoter. As such, measurements may be misidentified, meaning that certain collision events may have been obscured.

By using a template with an end-label, such as a DNA stem–loop described here, much greater insight into collision events between convergently aligned or tandomly oriented promoters could be obtained; indeed, the technique could be applied to study a range of DNA–protein interactions. By using our approach it will be possible to study more complicated systems involving a number of different proteins all associated with a single DNA stand, and to investigate directional processes on linear DNA templates in more detail.

ACKNOWLEDGEMENTS

We thank C. Rivetti for the kind gift of the pDSU template.

FUNDING

The Engineering and Physical Science Research Council through a doctoral training centre for the physical science–life science interface (DJB, PhD studentship). Funding for open access charge: The Engineering and Physical Science Research Council.

Conflict of interest statement. None declared.

REFERENCES

1. Alessandrini,A. and Facci,P. (2005) AFM: a versatile tool in biophysics. *Meas. Sci. Technol.*, **16**, R65–R92.
2. Hansma,H.G. (2001) Surface biology of DNA by atomic force microscopy. *Annu. Rev. Phys. Chem.*, **52**, 71–92.
3. Thomson,N.H. (2006) In: Bhushan,B., Fuchs,H. and Hosaka,S. (eds), *Applied Scanning Probe Methods Vol VI: Characterization*. Springer, Berlin.
4. Dame,R.T., Wyman,C. and Goosen,N. (2003) Insights into the regulation of transcription by scanning force microscopy. *J. Microsc.*, **212**, 244–253.
5. Davies,E., Teng,K.S., Conlan,R.S. and Wilks,S.P. (2005) Ultra-high resolution imaging of DNA and nucleosomes using non-contact atomic force microscopy. *FEBS Lett.*, **579**, 1702–1706.
6. Ellis,D.J., Dryden,D.T., Berge,T., Edwardson,J.M. and Henderson,R.M. (1999) Direct observation of DNA translocation and cleavage by the EcoKI endonuclease using atomic force microscopy. *Nat. Struct. Biol.*, **6**, 15–17.
7. Kasas,S., Thomson,N.H., Smith,B.L., Hansma,P.K., Miklossy,J. and Hansma,H.G. (1997) Biological applications of the AFM: from single molecules to organs. *Int. J. Imag. Syst. Technol.*, **8**, 151–161.
8. Montel,F., Castelnovo,M., Menoni,H., Angelov,D., Dimitrov,S. and Faivre-Moskalenko,C. (2010) RSC remodeling of oligo-nucleosomes: an atomic force microscopy study. *Nucleic Acids Res.*, **39**, 2571–2579.
9. Neaves,K.J., Cooper,L.P., White,J.H., Carnally,S.M., Dryden,D.T., Edwardson,J.M. and Henderson,R.M. (2009) Atomic force microscopy of the EcoKI Type I DNA restriction enzyme bound to DNA shows enzyme dimerization and DNA looping. *Nucleic Acids Res.*, **37**, 2053–2063.
10. Rees,W.A., Keller,R.W., Vesenka,J.P., Yang,G. and Bustamante,C. (1993) Evidence of DNA bending in transcription complexes imaged by scanning force microscopy. *Science*, **260**, 1646–1649.
11. Rivetti,C., Codeluppi,S., Dieci,G. and Bustamante,C. (2003) Visualizing RNA extrusion and DNA wrapping in transcription elongation complexes of bacterial and eukaryotic RNA polymerases. *J. Mol. Biol.*, **326**, 1413–1426.
12. Rivetti,C., Guthold,M., Sankar,L.A. and Susan,G. (2003) *Methods Enzymol*, Vol. 371. Academic Press, pp. 34–50.
13. Rippe,K., Guthold,M., von Hippel,P.H. and Bustamante,C. (1997) Transcriptional activation via DNA-looping: visualization of intermediates in the activation pathway of E. coli RNA polymerase x sigma 54 holoenzyme by scanning force microscopy. *J. Mol. Biol.*, **270**, 125–138.
14. Rivetti,C., Guthold,M. and Bustamante,C. (1999) Wrapping of DNA around the E.coli RNA polymerase open promoter complex. *EMBO J.*, **18**, 4464–4475.
15. Kasas,S., Thomson,N.H., Smith,B.L., Hansma,H.G., Zhu,X., Guthold,M., Bustamante,C., Kool,E.T., Kashlev,M. and Hansma,P.K. (1997) Escherichia coli RNA polymerase activity observed using atomic force microscopy. *Biochemistry*, **36**, 461–468.
16. Garcia,R. and Perez,R. (2002) Dynamic atomic force microscopy methods. *Surf. Sci. Rep.*, **47**, 197–301.
17. Neish,C.S., Martin,I.L., Henderson,R.M. and Edwardson,J.M. (2002) Direct visualization of ligand-protein interactions using atomic force microscopy. *Br. J. Pharmacol.*, **135**, 1943–1950.
18. Niemeyer,C.M., Adler,M., Pignataro,B., Lenhert,S., Gao,S., Chi,L., Fuchs,H. and Blohm,D. (1999) Self-assembly of DNA-streptavidin nanostructures and their use as reagents in immuno-PCR. *Nucleic Acids Res.*, **27**, 4553–4561.
19. Seong,G.H., Yanagida,Y., Aizawa,M. and Kobatake,E. (2002) Atomic force microscopy identification of transcription factor NFkappaB bound to streptavidin-pin-holding DNA probe. *Anal. Biochem.*, **309**, 241–247.
20. Shaiu,W.L., Larson,D.D., Vesenka,J. and Henderson,E. (1993) Atomic force microscopy of oriented linear DNA molecules labeled with 5nm gold spheres. *Nucleic Acids Res.*, **21**, 99–103.
21. Crampton,N. (2006). Convergent transcription studied by atomic force microscopy, PhD thesis, University of Leeds, Leeds, pp. 98–99.
22. Rivetti,C., Guthold,M. and Bustamante,C. (1996) Scanning force microscopy of DNA deposited onto mica: equilibration versus kinetic trapping studied by statistical polymer chain analysis. *J. Mol. Biol.*, **264**, 919–932.
23. Shlyakhtenko,L.S., Lushnikov,A.Y., Miyagi,A. and Lyubchenko,Y.L. (2012) Specificity of Binding of Single-Stranded DNA-Binding Protein to Its Target. *Biochemistry*, **51**, 1500–1509.
24. Escudé,C., Roulon,T., Lyonnais,S. and Le Cam,E. (2007) Multiple topological labeling for imaging single plasmids. *Anal. Biochem.*, **362**, 55–62.
25. Géron-Landre,B., Roulon,T. and Escude,C. (2005) Stem-loop oligonucleotides as tools for labelling double-stranded DNA. *FEBS J.*, **272**, 5343–5352.
26. Maxwell,A., Burton,N.P. and O'Hagan,N. (2006) High-throughput assays for DNA gyrase and other topoisomerases. *Nucleic Acids Res.*, **34**, e104.
27. Zuker,M. (2003) Mfold web server for nucleic acid folding and hybridization prediction. *Nucleic Acids Res.*, **31**, 3406–3415.
28. Crampton,N., Bonass,W.A., Kirkham,J., Rivetti,C. and Thomson,N.H. (2006) Collision events between RNA polymerases in convergent transcription studied by atomic force microscopy. *Nucleic Acids Res.*, **34**, 5416–5425.
29. Ohta,T., Nettikadan,S., Tokumasu,F., Ideno,H., Abe,Y., Kuroda,M., Hayashi,H. and Takeyasu,K. (1996) Atomic force microscopy proposes a novel model for stem-loop structure that binds a heat shock protein in the Staphylococcus aureus HSP70 operon. *Biochem. Biophys. Res. Commun.*, **226**, 730–734.
30. Yoshimura,S.H., Maruyama,H., Ishikawa,F., Ohki,R. and Takeyasu,K. (2004) Molecular mechanisms of DNA end-loop formation by TRF2. *Genes Cells*, **9**, 205–218.
31. Bustamante,C., Guthold,M., Zhu,X. and Yang,G.L. (1999) Facilitated target location on DNA by individual Escherichia coli RNA polymerase molecules observed with the scanning

force microscope operating in liquid. *J. Biol. Chem.*, **274**, 16665–16668.
32. Crampton,N., Yokokawa,M., Dryden,D.T., Edwardson,J.M., Rao,D.N., Takeyasu,K., Yoshimura,S.H. and Henderson,R.M. (2007) Fast-scan atomic force microscopy reveals that the type III restriction enzyme EcoP15I is capable of DNA translocation and looping. *Proc. Natl Acad. Sci. USA*, **104**, 12755–12760.
33. Crampton,N., Thomson,N.H., Kirkham,J., Gibson,C.W. and Bonass,W.A. (2006) Imaging RNA polymerase-amelogenin gene complexes with single molecule resolution using atomic force microscopy. *Eur. J. Oral Sci.*, **114**, 133–138; discussion 164–165.
34. Crampton,N., Roes,S., Dryden,D.T., Rao,D.N., Edwardson,J.M. and Henderson,R.M. (2007) DNA looping and translocation provide an optimal cleavage mechanism for the type III restriction enzymes. *EMBO J.*, **26**, 3815–3825.